Pure Appl. Chem., Vol. 71, No. 9, pp. 1717–1725, 1999.
Printed in Great Britain.

Solution structure of paramagnetic metalloproteins*

Ivano Bertini†, Antonio Rosato and Paola Turano

Department of Chemistry and Centro di Risonanze Magnetiche, University of Florence, Via L. Sacconi 6, 50019 Sesto Fiorentino, Italy

Abstract: Paramagnetism causes broadening of the NMR lines and therefore makes difficult the detection of the constraints (NOEs and ^{3}J) which are necessary for the determination of solution structures. The broadening is due to the fast nuclear relaxation rates, which are induced by the coupling of the nucleus with the unpaired electrons. Nevertheless, an NMR methodology has been developed, allowing the detection of classical constraints. This has allowed us to solve the first solution structure of a paramagnetic metalloprotein in 1994. Since then, several solution structures of paramagnetic proteins have appeared. In addition, paramagnetism has been exploited in order to obtain new, nonclassical constraints. First, the nuclear relaxation has been exploited to obtain metal–proton distances. The position of nuclei with respect to the magnetic susceptibility tensor axes has been determined by the use of pseudocontact shifts. The contact shifts have been used as constraints after discovering or confirming the shift dependence on dihedral angles. Paramagnetic molecules can be strongly magnetically anisotropic and therefore display partial orientation in strong external magnetic fields. These orientational effects result in dipolar contributions to the ^{15}N-^{1}H ^{1}J coupling. Such contributions can yield powerful structural constraints. In summary, the solution structure of many paramagnetic metalloproteins has been solved and described, and several new strategies have been developed for such solution structure determinations.

INTRODUCTION

The scientific community is facing the discovery of a very high number of protein sequences as a consequence of genome sequencing projects. In the gene bank <http://www.ncbi.nlm.nih.gov/Entrez/Genome/org.html> the complete sequences of the genome of 22 bacteria and archea, and 2 eukaryota are available. A simple genome like that of *E. coli* consists of 4639 221 base pairs, and contains 4288 protein-coding genes (87.8% of the genome). The average size of these proteins is 317 amino acids ($\approx$ 35 000 Da) [1]. These proteins, which are central to the biochemistry of life, should be structurally characterized. The structure of a protein can be solved through X-ray crystallography or through NMR spectroscopy. In the latter case these is the severe limitation of the low limit of molecular weights accessible (about 35 000 Da [2]), but there is the advantage of determining the structure in an environment similar to the physiological one and of being able to monitor the interaction of the protein with other biomolecules, as well as its mobility.

The solution structure is obtained by measuring a sufficient number of proton–proton distances and of protein dihedral angles [3]. From the known primary structure, computer programs generate a random 3D structure, which is adjusted until it satisfies all the experimental structural constraints within a given tolerance, yielding the solution structure [4,5]. If another structure is calculated starting from a different randomly generated structure, it will be different from the previous one, to a degree depending on the tolerance and the number of constraints used. In general it is preferred to have a large number of constraints and to use a relatively large tolerance in order to minimize the effects of possible problems in

* Plenary lecture presented at the 26th International Conference on Solution Chemistry, Fukuoka, Japan, 26–31 July 1999, pp. 1691–1764.
† *Corresponding author:* E-mail: bertini@cerm.unifi.it

the calibration of the constraints. As a result, a family of conformers is obtained whose root mean square deviation (RMSD) of the atom coordinates, calculated after best fitting, tells us what is the resolution of the structure. The local RMSD value varies along the polypeptide chain. High local RMSD values can be due to the lack of experimental constraints, to actual disorder of the structure in solution or both.

THE CASE OF METALLOPROTEINS

Metalloproteins, which are a significant share of the total, can be paramagnetic or diamagnetic. The metal nucleus can be studied by NMR only if it is magnetically active and sensitive enough. This is the case for ^{195}Pt, ^{113}Cd, ^{199}Hg, etc. for which HETCOR spectroscopy can provide information on the donor moieties [6–11]. Important metals like Ca and Zn are magnetically inactive and insensitive, respectively.

Common paramagnetic metal ions are Fe^{3+} and Cu^{2+}, which occur naturally, Co^{2+}, which can substitute Zn^{2+} in zinc-containing metalloproteins [12], and lanthanides, which can substitute Ca^{2+} in calcium-containing metalloproteins [13–15]. They have unpaired electrons, which cause enhancements in nuclear relaxation and tend to hamper the detection of the connectivities among nuclei, which are necessary for the obtainment of structural constraints. Few laboratories in the world are engaged in overcoming these drawbacks and in developing NMR experiments tailored for paramagnetic molecules. As a result of these efforts, several systems containing the above metal ions can be painfully investigated, whereas Mn^{2+} containing proteins are still prohibitive. The feasibility of NMR spectroscopy essentially depends on the electron relaxation times, which are long for the last metal ion (of the order of 10^{-8} s). High resolution NMR is only feasible when the paramagnetic metal ion has short electron relaxation times (roughly in the 10^{-10}–10^{-12} s range) [16,17].

Actually, the nuclear relaxation enhancements and the paramagnetic contribution to the chemical shift generated by unpaired electrons can be used to obtain further structural constraints. The first solution structure of a paramagnetic metalloproteins appeared in 1994 [18] and was further refined in the following years [19–21]. The protein contains a $[Fe_4S_4]^{2+}$ cluster, which is slightly paramagnetic (μ_{eff} per Fe 0.85 BM) [22], but the protons of the metal-coordinated cysteines relax very fast (the β protons have T_1s of the order of 5–10 ms) [23]. About 13 meaningful NOEs per residue were obtained together with a total of 45 constraints for the backbone ϕ dihedral angle (from $^3J_{HNH\alpha}$ and $^3J_{HNC'}$ values), and 26 constraints for the side chain χ_1 dihedral angle (from $^3J_{H\alpha H\beta}$ and $^3J_{NH\beta}$ values) [21]. Dihedral angle constraints were estimated also for the Fe-Sγ-Cβ-Hβ moieties, according to the following equation [24]

$$\delta^{hyp} = a \sin^2 \theta + b \cos \theta + c \quad (1)$$

Where δ^{hyp} is the hyperfine shift of the Hβ protons of the metal-coordinated cysteines, $a = 10.3 \pm 0.9$, $b = -2.2 \pm 0.4$ and $c = 3.9 \pm 0.5$ [25]. The values of *a, b* and *c* were determined by best fitting the δ^{hyp} observed for a number of $[Fe_4S_4]^{2+}$-containing proteins to the dihedral angle values measured in the corresponding solution or solid state structure [24,25]. Finally, 58 constraints based on the nuclear relaxation enhancement were included after a critical evaluation [21]. The longitudinal relaxation rate enhancement of the I-th proton, R_I, is proportional to the sixth power of the reciprocal distance between the nucleus and the *n*-th iron ion (r_{In}) [26]:

$$R_I = K \sum_{n=1}^{4} \frac{1}{r_{In}^6} \quad (2)$$

where the summation is extended to all the metal ions. *K* is a constant whose value is empirically obtained through calibration. It should be noted that in the present case all Fe ions are equivalent [27] and thus only one *K*-value is needed. More generally, each paramagnetic metal ion will have a different *K*-value [28]. The experimental nuclear relaxation rate is the sum of the above mentioned paramagnetic contribution (Eqn 2) plus a diamagnetic contribution [21,29,30]. A procedure was suggested to estimate the average diamagnetic contribution, which is subtracted from the experimental rate. The results were analyzed through a relaxation matrix method [30]. It was found that for geminal protons experiencing a large R_I contribution, Eqn 2 may not hold strictly because of cross relaxation [31,32], but the error induced in structure calculations is negligible for the majority of protons [30]. For structure calculations, some Fe-Fe and Fe-S distances had to be taken from structures determined through X-ray crystallography (Table 1). The obtained family of conformers was then refined through MD [33].

Table 1 Geometric parameters derived from X-ray data used to define the polymetallic center in solution structure calculations of reduced *E. halophila* HiPIP I [18]

Parameter	Angle (deg)	Distance (Å)
Cβ-Sγ	–	1.81
Sγ-Fe	–	2.17
Fe-Sϵ	–	2.22 (± 0.10)
Sϵ-Sϵ	–	3.50 (± 0.10)
Fe-Fe	–	2.65 (± 0.10)
Sγ-Sγ	–	5.90 (± 0.20)
Cβ-Sγ-Fe	105.8	–
Sγ-Fe-Sϵ	114.0	–

Many Fe-S proteins have then been studied with similar procedures, including the HiPIP from *C. vinosum* [34,35], the Fe_8S_8 ferredoxin from *C. pasteurianum* [30,36], the Fe_7S_8 ferredoxin from *B. schlegelii* [25] and its artificial Fe_8S_8 derivative [37], some Fe_4S_4 [38–40] and Fe_2S_2 [41–43] ferredoxins, the rubredoxin from *C. pasteurianum* [44], and some mutants of the above proteins [45,46]. Many paramagnetic cytochromes have also been studied (recently reviewed in [47]). They bind one or more heme cofactors, containing a low spin iron(III) with one unpaired electron. In the idealized tetragonal symmetry they have the electron distribution reported in Fig. 1. However, the imidazole ligand is asymmetric and splits the two degenerate *d* orbitals. In this way the unpaired electron occupies one orbital or another depending on the orientation of the axial ligands. As a result a relationship, although complex, is expected between such orientation and the *g*-values, the magnetic susceptibility (χ) anisotropy, the principal directions of the corresponding tensors and the chemical shifts of the protons and carbons of the heme moiety. Such a relationship has been proposed for cytochromes having two histidines or one histidine and a cyanide ion as axial ligands [48].

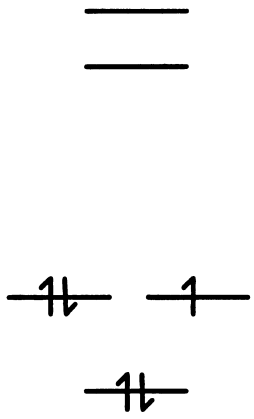

Fig. 1 *d* electron distribution for a low spin iron(III) complex in ideal tetragonal symmetry.

The occurrence of magnetic anisotropy causes the dipolar coupling between the electron and the resonating nucleus not to average to zero in solution [49]. This is because the electron magnetic moment changes with the orientation of the molecule with respect to the external magnetic field. This residual dipolar coupling provides a contribution to the nuclear chemical shift which is called pseudocontact shift (pcs). It is easily determined by measuring the chemical shift of the nuclei close to the iron but separated from it by enough chemical bonds that there is no unpaired electron spin density delocalized from the iron ion. To obtain the pcs values from these shifts it is necessary to subtract the corresponding shifts measured

in an otherwise identical diamagnetic analog. Pcs depend on the magnetic susceptibility anisotropy, and on the polar coordinates of the resonating nucleus with respect to the system of coordinates formed by the principal directions of the magnetic susceptibility tensor, according to the following equation [49]:

$$\delta^{\mathrm{pcs}} = \frac{1}{12\pi r_i^3}\left[\Delta\chi_{ax}^{metal}(3\cos^2\theta_i - 1) + \frac{3}{2}\Delta\chi_{rh}^{metal}(\sin^2\theta_i \cos 2\phi_i)\right] \quad (3)$$

where $\Delta\chi_{ax}^{metal}$ and $\Delta\chi_{rh}^{metal}$ are the axial and the rhombic anisotropies of the magnetic susceptibility tensor of the metal ion (χ^{metal}), r_i is the distance of the nucleus i from the metal ion, and θ_i and ϕ_i are polar coordinates describing the position of the observed nucleus in the axis system of the above tensor. Pcs are precious long-range constraints. As shown in Fig. 2, pcs allow a better refinement of the structure; indeed one more α-helix is observed in the structure of oxidized horse heart cytochrome *c* (the constraints used to obtain the structure are summarized in Table 2), which was not regularly folded without pcs constraints [50]. Furthermore, pcs allow the framing of the metal ion inside the protein part (Fig. 3). Protocols are available for the use of pcs in solution structure determination [51–53].

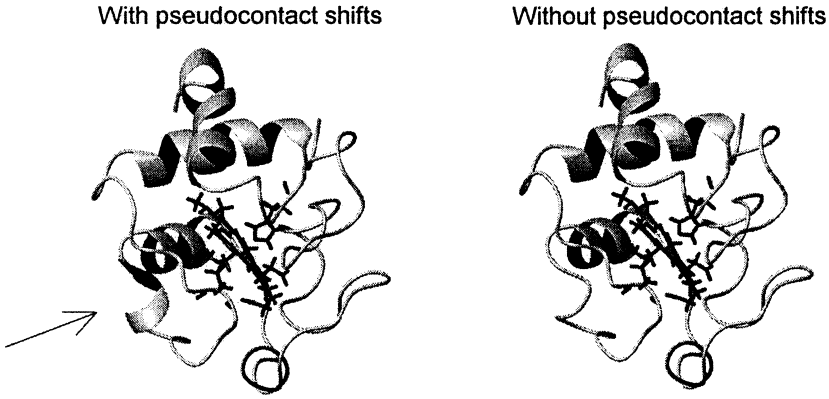

Fig. 2 Average solution structure of horse heart cytochrome c calculated with and without pseudocontact shifts [50].

Table 2 Constraints used in the solution structure calculations of horse heart ferricytochrome *c* [50]. The number of meaningful NOESY constraints is given in parentheses

Type of constraint	Number of constraints
2D NOESY	2250 (1729)
1D NOE	28
Pseudocontact shifts	241
H-bonds	14

As a result of the application of pcs, information on the magnetic susceptibility tensor of the metal (χ^{metal}) is obtained. In Fig. 4 the principal directions of the magnetic susceptibility tensor are shown for horse heart cytochrome c, together with the anisotropy values [50]. The occurrence of magnetic anisotropy implies that the molecular tumbling in solution is not random anymore at high magnetic fields. Instead, a partial orientation occurs [54,55]. This provides dipolar couplings between nuclei values different from zero: they are called residual dipolar couplings (rdc). They can be detected conveniently by measuring ^{15}N-^{1}H ^{1}J values at variable magnetic fields [56]. Since the partial orientation depends on the square of the external magnetic field, then the dipolar contribution to the ^{15}N-^{1}H coupling will vary accordingly [56,57]. A study is available for oxidized rat cytochrome b_5 [58]. Differences between the

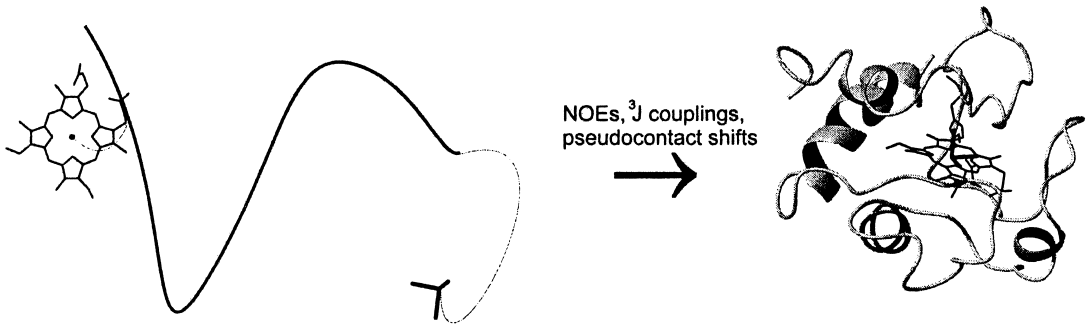

Fig. 3 A schematic representation of structure calculations run using classical constraints together with pseudocontact shifts for heme containing proteins. The position of the metal ion is represented by the origin of the Cartesian reference system constituted by the magnetic anisotropy tensor, which is linked to the polypeptide chain (thick line) by a chain of pseudo-atoms with a null Van der Waals radius (narrow line). A similar chain is also used to link the heme moiety to the polypeptide.

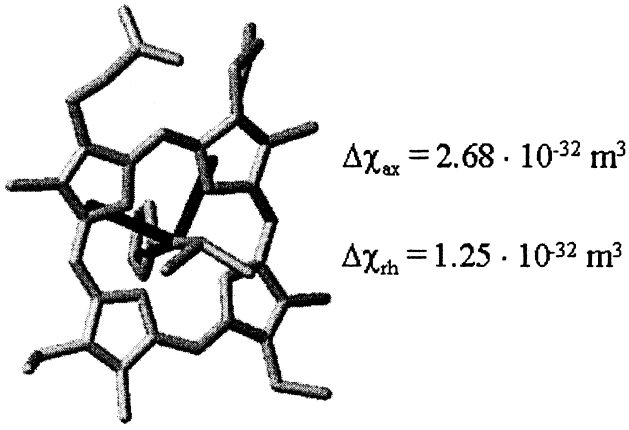

Fig. 4 Principal directions and anisotropy values for the metal magnetic susceptibility tensor in oxidized horse heart cytochrome *c* [50].

^{15}N-^{1}H ^{1}J couplings measured at 500 and 800 MHz as large as ≈ 1 Hz were experimentally found. This allowed us to obtain an alignment tensor and the orientation of each N-H vector in the system of coordinates of the alignment tensor through the following equation [56–58]:

$$\Delta rdc(Hz) = -\frac{1}{4\pi}\frac{\Delta B_0^2}{15kT}\frac{\gamma_H\gamma_N h}{4\pi^2 r_{HN}^3}\left[\Delta\chi_{ax}^{mol}(3\cos^2\theta_i - 1) + \frac{3}{2}\Delta\chi_{rh}^{mol}(\sin^2\theta_i\cos^2\phi_i)\right] \quad (4)$$

where $\Delta\chi_{ax}^{mol}$ and $\Delta\chi_{rh}^{mol}$ are the axial and rhombic anisotropies of the alignment tensor (χ^{mol}), and θ_i and ϕ_i are polar coordinates describing the orientation of the *i*-th N–H bond vector in the axis system of the alignment tensor. The structural constraints actually used are the *differences* between values at two different fields (Δrdc). Actually, Eqn 4, which is similar to Eqn 3, is used for structure determination. Here ^{15}N-^{1}H ^{1}J values must be corrected for the field dependence of the dynamic frequency shift of ^{15}N, which also concurs to the determination of the measured ^{1}J value [57]. NOEs, PCS and ^{15}N–^{1}H Δrdc constraints are compatible, and can be used simultaneously as shown in Table 3. The addition of a set of constraints does not induce any significant increase of the violations in the other set of constraints. As a result of the use of ^{15}N-^{1}H rdc, the alignment tensor is obtained, which is just the molecular magnetic anisotropy ($\Delta\chi^{mol}$). This is different from the magnetic anisotropy obtained from the use of pcs, which is due only to the metal ($\Delta\chi^{metal}$). χ^{mol} is the sum of χ^{metal} plus χ^{dia}, where the latter parameter is the magnetic susceptibility tensor of the diamagnetic molecule. $\Delta\chi^{dia}$ was experimentally obtained by performing the same measurements on reduced cytb5 [58]. Here the magnetic anisotropy is essentially

Table 3 Number of constraints and constraint violation statistics relative to calculations of the solution structure of reduced and oxidized cytochrome b_5 run using different sets of constraints [58]. The number of meaningful distance constraints is given in parentheses

	Reduced	Reduced	Oxidized	Oxidized	Oxidized
Number of contraints					
Distance constraints	1722 (1203)	1722 (1203)	1810 (1372)	1810 (1372)	1810 (1372)
Pseudocontact shifts	n.a.	n.a.	0	235	235
Residual dipolar couplings	0	55	0	0	62
Constraint violations					
Average violation per NOE constraint (Å)	0.0041 ± 0.0005	0.0040 ± 0.0005	0.0017 ± 0.0002	0.0028 ± 0.0004	0.0033 ± 0.0005
Average deviation per Δrdc constraint (Hz)	0.07 ± 0.01	0.025 ± 0.006	0.17 ± 0.12	0.19 ± 0.14	0.021 ± 0.002
Average deviation per pcs constraint (p.p.m.)	n.a.	n.a.	0.3 ± 1.1	0.029 ± 0.005	0.04 ± 0.02

n.a.: not applicable.

due to the ring current of the heme, and to the C(O)NH moieties, whose anisotropies in helices sum up. Indeed, cytb5 has four almost parallel helices, whose axis is nearly parallel to the heme plane. The anisotropy values and principal directions of χ^{mol}, χ^{metal} and χ^{dia} are reported in Fig. 5 [58].

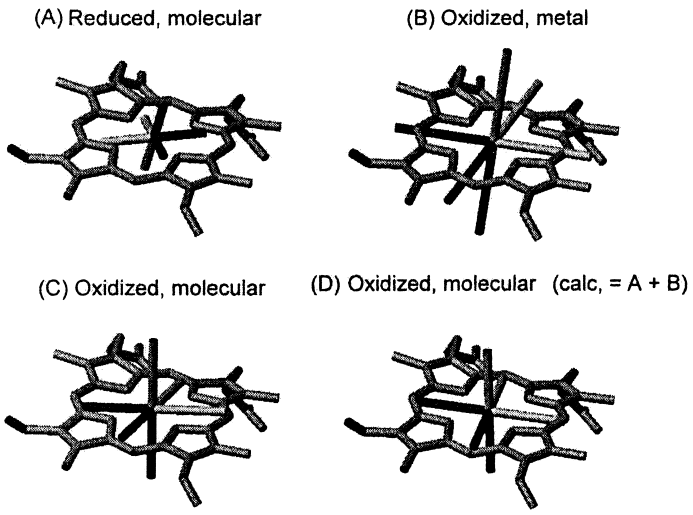

Fig. 5 Molecular and metal magnetic susceptibility tensors measured for reduced and oxidized cytochrome b_5 [58]. Magnetic anisotropy values are as follows: (A) $\Delta\chi_{ax} = -0.8\times10^{-32}$ m^3, $\Delta\chi_{rh} = 0.1\times10^{-32}$ m^3, (B) $\Delta\chi_{ax} = 2.8\times10^{-32}$ m^3, $\Delta\chi_{rh} = -1.1\times10^{-32}$ m^3, (C) $\Delta\chi_{ax} = 2.2\times10^{-32}$ m^3, $\Delta\chi_{rh} = -1.3\times10^{-32}$ m^3, (D) $\Delta\chi_{ax} = 2.1\times10^{-32}$ m^3, $\Delta\chi_{rh} = -1.0\times10^{-32}$ m^3. The length of the axes reflects the relative values of $\Delta\chi_{ax}$. The tonality of the axes in (A) is inverted to show pictorially that $\Delta\chi_{ax}$ has opposite sign with respect to the other tensors.

CONCLUDING REMARKS

It is shown here that it is possible to solve the solution structure of paramagnetic metalloproteins, provided that the linewidth is not too severely affected. In this case new constraints can be used, which are based on the resonating nucleus-unpaired electron(s) interaction, and allow the localization of the metal ion within the protein frame. The observability of the NMR signals depends on the electron relaxation times, which on their turn are determined by the nature of the metal ion and of the ligands [16,17]. Its understanding is of course of help. For example, tetrahedral cobalt(II) provides broad NMR lines, whereas octahedral cobalt(II) provides sharp lines [16]. Copper(II) in blue copper proteins can be affordable, whereas the same ion in type II coordination becomes prohibitive [16,59]. Polymetallic centers often have favorable electronic relaxation times, and therefore ferredoxins are more easily amenable to NMR investigation than rubredoxins, which contain a single iron ion [17,60].

REFERENCES

1 F. R. Blattner, G. Plunkett, C. A. Bloch, N. T. Perna, V. Burland, M. Riley, J. Collado-Vides, J. D. Glasner, C. K. Rode, G. F. Mayhew, J. Gregor, N. W. Davis, H. A. Kirkpatrick, M. A. Goeden, D. J. Rose, B. Mau, Y. Shao. *Science* **277,** 1453–1474 (1997).

2 G. M. Clore, A. M. Gronenborn. In *Encyclopedia of Nuclear Magnetic Resonance* (D. M. Grant, R. K. Harris, eds), pp. 4602–4622. John Wiley & Sons, Chichester, UK (1996).

3 K. Wüthrich. *NMR of Proteins Nucleic Acids*. Wiley, New York (1986).

4 A. T. Brunger, P. D. Adams, G. M. Clore, W. L. DeLano, P. Gros, R. W. Grosse-Kunstleve, J. S. Jiang, J. Kuszewski, M. Nilges, N. S. Pannu, R. J. Read, L. M. Rice, T. Simonson, G. L. Warren. *Acta Crystallogr. D Biol. Crystallogr.* **54,** 905–921 (1998).

5 P. Güntert, C. Mumenthaler, K. Wüthrich. *J. Mol. Biol.* **273,** 283–298 (1997).

6 J. D. Otvos, H. R. Engeseth, S. Wehrli. *J. Magn. Reson.* **61,** 579–584 (1985).

7 D. H. Live, L. K. Christopher, D. Cowburn, J. L. Markley. *J. Am. Chem. Soc.* **107,** 3043–3045 (1985).

8 T. Pan, J. E. Coleman. *Proc. Natl. Acad. Sci. USA* **87,** 2077–2081 (1990).

9 J. E. Coleman. *Meth Enzymol.* **227,** 16–43 (1993).

10 K. H. Gardner, J. E. Coleman. *J. Biomol. NMR* **4,** 761–774 (1994).

11 L. M. Utschig, J. W. Bryson, T. V. O'Halloran. *Science* **268,** 380–385 (1995).

12 L. Banci, M. Piccioli. In *Encyclopedia of Magnetic Resonance* (D. M. Grant, R. K. Harris, eds), pp. 1365–1373. John Wiley & Sons, Chichester, UK (1996).

13 L. Lee, B. D. Sykes. *Biochemistry* **22,** 4366–4373 (1983).

14 F. Capozzi, M. A. Cremonini, C. Luchinat, M. Sola. *Magn. Reson. Chem.* **31,** S118–S127 (1993).

15 D. Bentrop, I. Bertini, M. A. Cremonini, S. Forsén, C. Luchinat, A. Malmendal. *Biochemistry* **36,** 11605–11618 (1997).

16 I. Bertini, C. Luchinat. *NMR of paramagnetic molecules in biological systems*. Benjamin/Cummings, Menlo Park, CA (1986).

17 I. Bertini, C. Luchinat. *NMR of Paramagnetic Substances*, p. 1. Coord. Chem. Rev. 150. Elsevier, Amsterdam (1996).

18 L. Banci, I. Bertini, L. D. Eltis, I. C. Felli, D. H. W. Kastrau, C. Luchinat, M. Piccioli, R. Pierattelli, M. Smith. *Eur. J.Biochem.* **225,** 715–725 (1994).

19 I. Bertini, A. Donaire, I. C. Felli, C. Luchinat, A. Rosato. *Magn. Reson. Chem.* **34,** 948–950 (1996).

20 I. Bertini, I. C. Felli, C. Luchinat, A. Rosato. *Proteins Struct. Funct. Genet.* **24,** 158–164 (1996).

21 I. Bertini, M. M. J. Couture, A. Donaire, L. D. Eltis, I. C. Felli, C. Luchinat, M. Piccioli, A. Rosato. *Eur. J.Biochem.* **241,** 440–452 (1996).

22 W. D. Phillips, C. C. McDonald, N. A. Stombaugh, W. H. Orme-Johnson. *Proc. Natl. Acad. Sci. USA* **71,** 140–143 (1974).

23 I. Bertini, I. C. Felli, D. H. W. Kastrau, C. Luchinat, M. Piccioli, M. S. Viezzoli. *Eur. J. Biochem.* **225,** 703–714 (1994).

24 I. Bertini, F. Capozzi, C. Luchinat, M. Piccioli, A. J. Vila. *J. Am. Chem. Soc.* **116,** 651–660 (1994).

25 S. Aono, D. Bentrop, I. Bertini, A. Donaire, C. Luchinat, Y. Niikura, A. Rosato. *Biochemistry* **37,** 9812–9826 (1998).

26 I. Solomon. *Phys. Rev.* **99,** 559–565 (1955).

27 P. Middleton, D. P. E. Dickson, C. E. Johnson, J. D. Rush. *Eur. J. Biochem.* **104,** 289–296 (1980).

28 I. Bertini, A. Donaire, I. C. Felli, C. Luchinat, A. Rosato. *Inorg. Chem.* **36,** 4798–4803 (1997).

29 J. G. Huber, J.-M. Moulis, J. Gaillard. *Biochemistry* **35,** 12705–12711 (1996).

30 I. Bertini, A. Donaire, C. Luchinat, A. Rosato. *Proteins Struct. Funct. Genet.* **29,** 348–358 (1997).

31 J. Granot. *J. Magn. Reson.* **49,** 257–270 (1982).

32 G. N. La Mar, J. S. de Ropp. In *Biological Magnetic Resonance* (L. J. Berliner, J. Reuben, eds), Vol. 12, pp. 1–78. Plenum Press, New York (1993).

33 D. A. Pearlman, D. A. Case, J. W. Caldwell, W. S. Ross, T. E. Cheatham, D. M. Ferguson, G. L. Seibel, U. C. Singh, P. K. Weiner, P. A. Kollman. *AMBER 5.0*, University of California, San Francisco (1997).

34 L. Banci, I. Bertini, A. Dikiy, D. H. W. Kastrau, C. Luchinat, P. Sompornpisut. *Biochemistry* **34,** 206–219 (1995).

35 I. Bertini, A. Dikiy, D. H. W. Kastrau, C. Luchinat, P. Sompornpisut. *Biochemistry* **34,** 9851–9858 (1995).

36 I. Bertini, A. Donaire, B. A. Feinberg, C. Luchinat, M. Piccioli, H. Yuan. *Eur. J. Biochem.* **232,** 192–205 (1995).

37 S. Aono, D. Bentrop, I. Bertini, G. Cosenza, C. Luchinat. *Eur. J. Biochem.* **258,** 502–514 (1998).

38 P. L. Wang, A. Donaire, Z. H. Zhou, M. W. W. Adams, G. N. La Mar. *Biochemistry.* **35,** 11319–11328 (1996).

39 H. Sticht, G. Wildegger, D. Bentrop, B. Darimont, R. Sterner, P. Roesch. *Eur. J. Biochem.* **237,** 726–735 (1996).

40 S. L. Davy, M. J. Osborne, G. R. Moore. *J. Mol. Biol.* **277,** 683–706 (1998).

41 C. Lelong, P. Sétif, H. Bottin, F. André, J.-M. Neumann. *Biochemistry* **34,** 14462–14473 (1995).

42 H. Hatanaka, R. Tanimura, S. Katoh, F. Inagaki. *J. Mol. Biol.* **268,** 922–933 (1997).

43 I. Sang-Choul, G. Liu, C. Luchinat, A. G. Sykes, I. Bertini. *Eur. J. Biochem.* **258,** 465–477 (1998).

44 I. Bertini, D. M. Kurtz Jr, M. K. Eidsness, G. Liu, C. Luchinat, A. Rosato, R. A. Scott. *JBIC* **3,** 401–410 (1998).

45 D. Bentrop, I. Bertini, F. Capozzi, A. Dikiy, L. D. Eltis, C. Luchinat. *Biochemistry* **35,** 5928–5936 (1996).

46 I. Bertini, M. Borsari, M. Bosi, L. D. Eltis, I. C. Felli, C. Luchinat, M. Piccioli. *JBIC* **1,** 257–263 (1996).

47 L. Banci, I. Bertini, C. Luchinat, P. Turano. In *The Porphyrin Handbook* (K. M. Kadish, K. M. Smith, R. Guilard, eds). Academic Press, Burlington, MA (1999).

48 I. Bertini, C. Luchinat, G. Parigi, F. A. Walker. *JBIC* **4**, 515–519 (1999).

49 H. M. McConnell, R. E. Robertson. *J. Chem. Phys.* **29,** 1361–1365 (1958).

50 L. Banci, I. Bertini, H. B. Gray, C. Luchinat, T. Reddig, A. Rosato, P. Turano. *Biochemistry* **36,** 9867–9877 (1997).

51 L. Banci, I. Bertini, K. L. Bren, M. A. Cremonini, H. B. Gray, C. Luchinat, P. Turano. *JBIC* **1,** 117–126 (1996).

52 L. Banci, I. Bertini, G. Gori Savellini, A. Romagnoli, P. Turano, M. A. Cremonini, C. Luchinat, H. B. Gray. *Proteins Struct. Funct. Genet.* **29,** 68–76 (1997).

53 L. Banci, I. Bertini, M. A. Cremonini, G. Gori Savellini, C. Luchinat, K. Wüthrich, P. Guentert. *J. Biomol. NMR* **12,** 553–557 (1998).

54 P. C. M. van Zijl, B. H. Ruessink, J. Bulthuis, C. Maclean. *Accounts Chem Research* **17,** 172–180 (1984).

55 A. A. Bothner-By. In *Encyclopedia of Nuclear Magnetic Resonance* (D. M. Grant, R. K. Harris, eds), pp. 2932–2938. John Wiley & Sons, Chichester, UK (1996).

56 J. R. Tolman, J. M. Flanagan, M. A. Kennedy, J. H. Prestegard. *Proc. Natl. Acad. Sci. USA* **92,** 9279–9283 (1995).

57 N. Tjandra, S. Grzesiek, A. Bax. *J. Am. Chem. Soc.* **118,** 6264–6272 (1996).

58 L. Banci, I. Bertini, J. G. Huber, C. Luchinat, A. Rosato. *J. Am. Chem. Soc.* **120,** 12903–12909 (1998).

59 I. Bertini, S. Ciurli, A. Dikiy, R. Gasanov, C. Luchinat, G. Martini, N. Safarov. *J. Am. Chem. Soc.* **121,** 2037–2046 (1999).

60 I. Bertini, C. Luchinat, A. Rosato. *Adv. Inorg. Chem.* **47,** 251–282 (1999).